Diameter sensor selection

Owen Lu
Electroimpact Inc.
owenl@electroimpact.com

***Abstract*—This document details the tests that were conducted on 3 different distance sensors that will be used for spool diameter sensing and inertia estimation on new AFP heads systems.**

I. Introduction

The reason tests are conducted is to evaluate the performance of the different sensors in terms of precision and accuracy in a realistic setting. Practical implementation issues, such as wiring difficulty will also be taken into account in the end qualitatively, although evaluation of this is not covered in this specific document.

II. Sensors

Of the three sensors, two are laser sensors, while one is an ultrasonic sensor. The family part numbers are listed below with hyperlinks:

1. Balluff BOD000N (Laser)
2. Leuze ODSL8 (Laser)
3. Balluff S004J (Ultrasonic)

III. Apparatus

Since servo spool research is being conducted simultaneously, the same test rig was used, a solid model representation is shown in Figure 1.

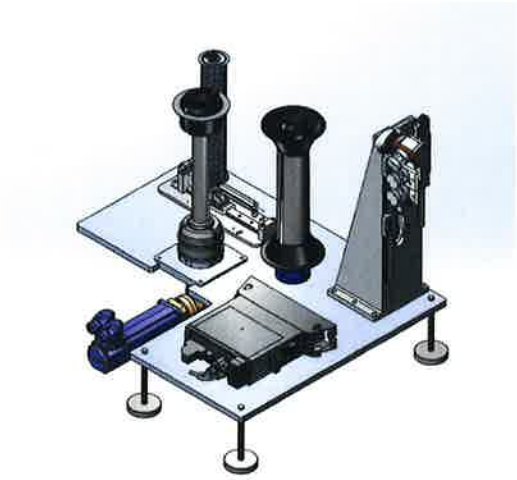

Figure 1- Solid model representation of test apparatus

The reason it is mounted to the test rig is so that the servo can rotate and the angular position of the output shaft can be recorded simultaneously with the diameter measurements.

IV. Procedure

The experimental procedure is listed below.

1. Connect sensor to Bosch IndraDrive
2. Mount spool of known diameter (measured via calipers)
3. Record input voltage
4. Mount second spool of known diameter (measured via calipers)
5. Record input voltage
6. Perform linear calibration for interpolation and extrapolation for diameter
7. Use Bosch IndraWorks oscilloscope function to record data (time, angular velocity, diameter reading)
8. Run step velocity input of 80RPM
9. Stop recording
10. Repeat 7-9 with 120, 160, and 200RPM
11. Repeat 1-10 with all sensors

V. Performance Metrics

The main metric in quantifying reliability taken into consideration as the maximum and minimum deviation in the time domain signal as recommended by Chris Connair.

Although each measurement is important, more importantly is the average of the measurements over one revolution. Of course the angular rate combined with the sampling rate T_s defines how many measurements can be taken over one revolution.

To calculate the number of samples n we can use Eq. (1) and (2).

$$T = \frac{2\pi}{\omega} \tag{1}$$

$$n = \max\left\{n \in \mathbb{Z}, n < \frac{T}{T_s}\right\} \tag{2}$$

The standard error of the measurement can be estimated with

$$SE_{\bar{x}} = \frac{s}{\sqrt{n}} \tag{3}$$

During the fastest payout of 1.69m/s with the smallest spool diameter of 3.5'' allows us to calculate the minimum theoretical n value based on given T_s.

$$\omega = 38rad/s$$
$$T = \frac{2\pi}{\omega} = 0.1653s$$

Therefore, 1000Hz sampling rate, would mean $n = 165$. An example calculation follows of how to estimate the 95% confidence interval of the mean value.

For the Balluff laser sensor, the standard deviation was measurement to be $s = 5.86mm$. This was by far the worst performing sensor of the three, and gives an upper bound of the expected standard error.

Therefore, $SE_{\bar{x}}$ can be calculated and the 95% confidence interval estimated.

$$SE_{\bar{x}} = \frac{5.86mm}{\sqrt{165}} = 0.4562mm$$
$$95\%\ CI \approx\ x - 2SE_{\bar{x}}, x + 2SE_{\bar{x}}$$

This means that with 95% confidence, the diameter of the spool can be estimated to within ~1mm assuming zero offset error. Knowing that this can estimate the magnitude of random error, it shows that all sensors are sufficient for the job.

Tabulated below are the results for the maximum and minimum along with the 95% confidence interval. The measured diameter using calipers was 95.4mm.

Sensor	95% CI (mm)	Min/Max (mm)
BOD000N	(94.4, 96.3)	(79.7, 105.0)
ODSL8	(95.0, 95.7)	(87.4, 99.2)
S004J	(95.2, 95.52)	(93.9, 96.5)

All sensors agree with the caliper measurements within their 95% confidence intervals and are suitable for the task. However, a construction of polar plots given time domain angular position and radius measurements allows us to see the clear winner instantly. Following are the polar constructions of the time domain diameter data in Figure 2.

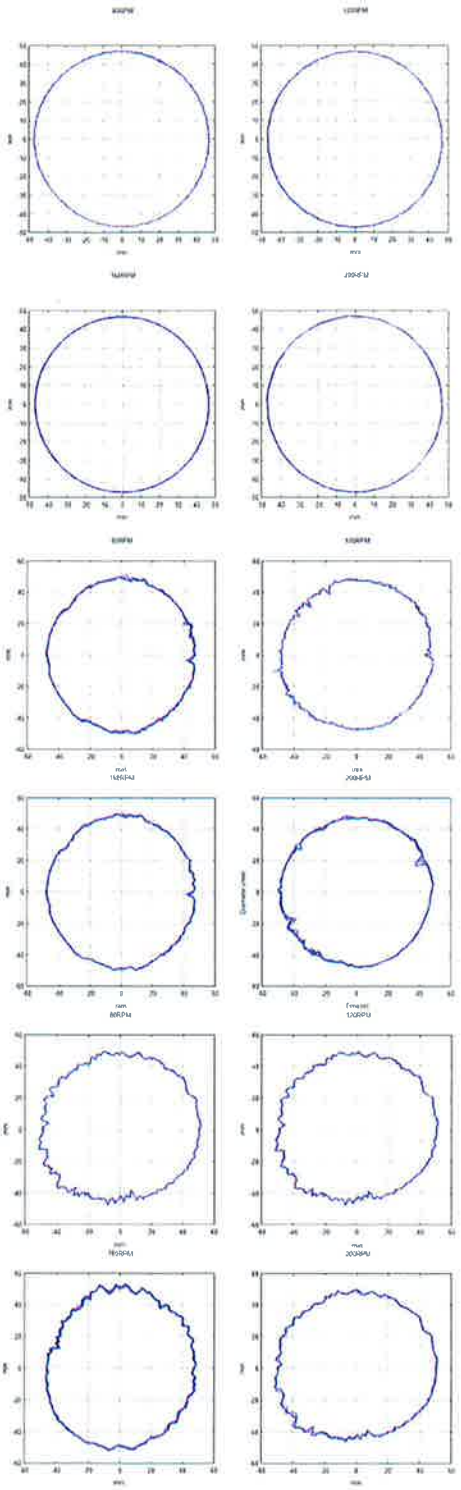

Figure 2 - Polar construction of spool; Ultrasonic (top), Leuze laser (middle), Balluff laser (bottom)

Real time gain tuning and inertia estimation

Owen Lu
Electroimpact Inc.
owenl@electroimpact.com

***Abstract*—This brief document describes the theoretical basis for inertia estimation from radius measurements. The inertia measurement is important for both high and low level controllers, since proportional gains can be increased to speed up the response while simultaneously operating within current limits of the motor.**

I. Introduction

The main problem is to generate rules to set proportional gain K_p based on radius measurements in real time. As the radius of the spool decreases, the open loop gain is effectively lowered, since the radius scales angular velocity for surface speed, thereby reducing the bandwidth of the closed loop system. However, as the radius decreases the inertia of the system also decreases, allowing the proportional gain to be increased to compensate the reduction in performance. We thus, attempt to develop a simple computationally inexpensive rule to ensure consistent performance across any spool diameter.

II. Inertia estimation

Previously weighing carbon spools and creating solid models with similar geometry and uniform density was used to estimate the inertia of the spool which is the main inertial element in the system. Interpolation methods were then used to estimate the inertia for any radius that lies within the range of modelled values.

Another simple method is to use a hollow cylinder geometry with uniform density to approximate the inertia.

$$I_{cyl} = \frac{1}{2}MR^2 \tag{1}$$

Assuming the carbon portion is uniform density and takes on the form of a hollow cylinder, the carbon inertia can then be approximated with the following method.

$$I_{cyl} = \frac{1}{2}MR^2 \tag{2}$$

$$I_{carbon} = \frac{1}{2}\rho\pi r^4 - \frac{1}{2}\rho\pi r_0^4 \tag{3}$$

The spindle, cardboard roll and other inertia elements are then lumped as a single constant I_0. Since the second term in the carbon fiber inertia is constant this will also be lumped into I_0.

$$I_{effective}(r) = I_0 + \frac{1}{2}\rho\pi r^4 \tag{4}$$

The quartic relationship with radius in (4) means that the inertia of the system will decrease rapidly as material is payed out. Notably, the plastic backing wrapping around the take up is neglected for simplicity.

III. Inertia calculation comparison

Using data provided by Kyle Jeffries, a curve fit was performed on the inertia approximations. The fit agrees with the current approximation method well and therefore will be used in the controller implementation.

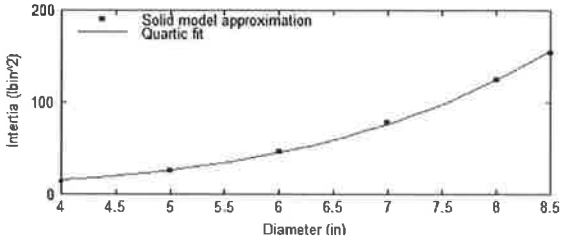

IV. Proportional gain re-tuning

In order to maintain the same overall disturbance rejection a simple condition is to be maintained.

$$K_p r_s = C_0 \tag{5}$$

Where C_0 is some constant

Therefore, suppose that initially the gain is set to its maximum when the inertia of the spool is largest using (6).

$$K_p = \frac{2T_m}{v_a I_e} \tag{6}$$

Then, C_0 can be calculated and an explicit formula used for K_p can be obtained. This ensures that the closed loop performance is the same throughout all radii. Thus, the update equation in the control loop is given in (7).

$$K_p = C_0 / r_s \tag{7}$$

Experimental Estimation of Loaded Spindle Inertia

Owen Lu
Electroimpact Inc.
owenl@electroimpact.com

***Abstract*—Previously 3D CAD models within Solidworks were used to estimate the inertia of the material spindle and carbon fiber spools. In order to verify the validity of the approximation, a simple experiment was done to approximate the inertia of the system at the output of the gearbox and subsequently calculate the spool inertia.**

I. Introduction

The effective inertia of the system is an extremely important quantity when sizing the motor. Approximating the inertia accurately reduces the risk of oversizing the motor and the other components in the system relevant to power delivery and energy dissipation.

II. Apparatus

The mechanical system is made up of the following components:

1. Elmo L60-48VDC Servo Motor
2. Harmonic HPG20 7:1 Reducer
3. Flange mount material spindle
4. Carbon fiber spool

III. Friction Modelling

In order to calculate the inertia, a model of friction was used which included the static and viscous elements.

$$T_{friction} = T_0 + T_v\omega, \omega \geq 0 \qquad (1)$$
$$T_{friction} = -T_0 + T_v\omega, \omega < 0$$

At this point, a curve fitting algorithm can be used to match the torques with measured values. The total torque at the input is the sum of the acceleration torque and the frictional torque expressed in Eq. 2.

$$T = T_{friction} + I_e\omega' \qquad (2)$$

Thus, three parameters must be minimized simultaneously, I_e, T_0, T_v to match the model torque to the measured torque.

IV. Measurement

In the interest of time, a sinusoidal wave was used for the velocity profile. Using Elmo's measurement system, the velocity and the current were measured over time with a 1ms sampling time.

After defining a sinusoidal velocity profile, the measured output of the system was determined by a least squares for a sinusoidal fit.

$$\omega(t) \approx 60.43\sin(59.43t + 1.989)rads^{-1} \qquad (3)$$

Below is a typical graph showing the relationship between the torque and the acceleration.

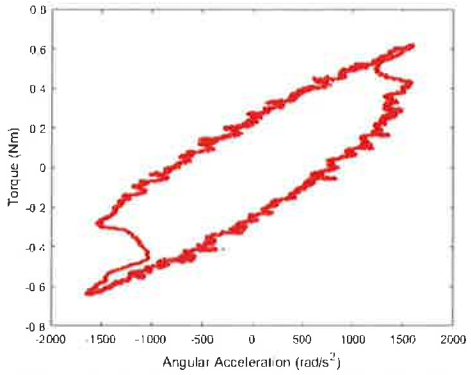

Figure 1 - Raw Torque vs. Angular Acceleration

As we expect the graph seems symmetric and the max and minimum torques are of the same magnitude. The oblong shape of the graph is due to the transition of the velocity from positive to negative combined with the viscous friction. At this point, the frictional torque used to drive the system reverses.

From the plot following, we can see the transition regions between the torque and the angular velocity as the direction of rotation is changed.

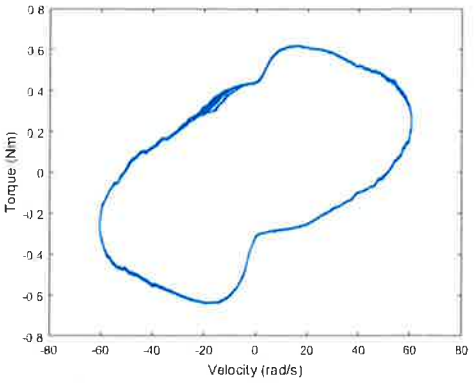

Figure 2 – Torque vs. Angular Velocity

V. Curve Fit

Using MATLAB's lsqcurvefit function the three parameters were estimated. The algorithm minimizes the 2-norm squared, which is a conventional least squares fit. In order to get a more accurate estimate, the low-velocity points were omitted. This due to the friction model inaccuracy near the zero velocity transition.

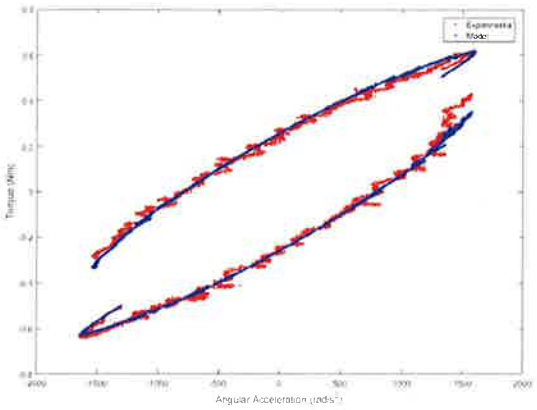

Figure 3 – Torque vs. Angular acceleration with fit

VI. Regression Verification

One last check to ensure the torques are accurately represented by the model was to compare the theoretical torque directly to the data. We expect a linear curve with zero y-intercept and slope of 1 in theory. This is verified in the figure below with $R^2 = 0.996$. The slope and intercept were estimated to be $(0.9962, -0.0021)$ respectively for a 4.6in spool.

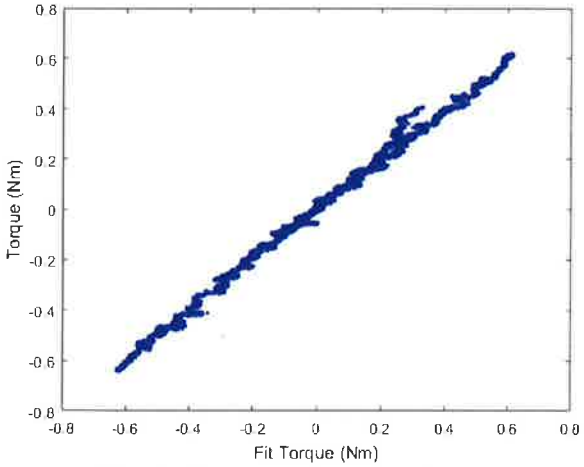

Figure 4 - Direct comparison of torques

In order to generate values for the inertia vs. radius of the spool, we can use documented values of the mechanical elements to the system and subtract them from the input inertia.

VII. Calculating Spool Output

In order to estimate the spool, an inertia model was created. The input inertia of the system at the input is the total of the rotor, gearbox, spindle and spool inertias. However, since a 7:1 reducer is present, the spindle and spool inertias are reduced by a factor of 49 for the effective inertia at the input. It is important to note that the spindle inertia includes that of the backing take-up spool since it is driven by the tow.

$$I_e = I_{rotor} + I_{gear} + \frac{I_s + I_{spool}}{49} \quad (4)$$

Using the estimate of I_e from the curve fits and documented values for the I_{rotor}, I_{gear}, I_s inertias, the spool inertia can be solved.

$$I_{spool} = 49(I_e - I_{rotor} - I_{gear}) - I_s \quad (5)$$

VIII. Results

Using Eq. 5 the spool inertias were calculated. Noticeably the 4.6inch spool had a calculated inertia of much less than expected from previous model based estimations. This is somewhat expected since larger spools are less prone to being skewed due to inertia estimation error.

Diameter (in)	Inertia (kgm^2)
4.6	0.0012
5.6	0.0089
8.4	0.056

IX. Possible Improvements

A simple improvement to. this experiment would be to use a sinusoidal velocity input superimposed on a constantly velocity signal. This would allow the velocity to be varied without changing the overall direction, effectively removing the effects of the transitional friction. A more accurate experiment would be to run the spools at multiple constant velocities and monitor the torque to generate the friction vs. speed curves. At this point then the inertia can be estimated with a known friction relationship. The reason three parameters were fit simultaneously with a sinusoidal input is purely due to the ease of obtaining reliable results in a timely fashion as sinusoidal waves can be generated easily from the EAS and a single recording could be imported for inertia calculation.

Low level controller design and trajectory generation

Owen Lu
Electroimpact Inc.
owenl@electroimpact.com

***Abstract*—The previous high level control design document describes how the torque requirements can be limited by selection of controller constants that smooth the velocity control signal. This paper documents how the lower level position, which outputs a torque command signal can be tuned to generate the desired results.**

I. Introduction

Of the three motors thoroughly investigated so far, the Moog Animatics motor has the best form factor, and best power density with all required I/O for the process. It is also unlikely that other companies have the same or similar functionality and form factor since Animatics has spent years on litigation to reduce competition. However, the software's lack of identification methods is a major weak point in the system and a theoretical basis is needed to verify the performance of the system as the dynamics evolve in order to develop robust tuning rules. Testing is thus done in order to verify the theoretical prediction of performance and the validity of using pre-tuned parameters in practice.

II. System Identification

In order to approximate the system, an assumption is made that the plant is second order. The reasoning is that the motor is sized to respond in the low bandwidth region where the current control loop is approximated as a constant gain. That is torque is assumed to be delivered instantly.

The plant then takes on the assumed form. The units of the constants J_e, B_e are scaled versions of inertia and damping. However, as far as identification, the exact units are not necessary.

$$P(s) = \frac{1}{J_e s^2 + B_e s}$$

The SmartMotor always operates in closed loop and thus, setting all constants to zero, other than proportional gain is represented in the control loop following.

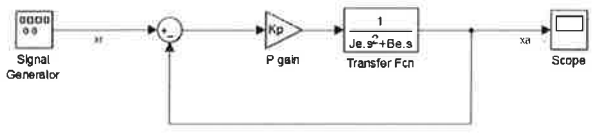

Figure 1 - Servo control loop model

The overall transfer function describing x_a/x_r is then a second order system. K_p in theory then can be adjusted until oscillation is observed in the signal.

This was verified using the SMITuner tool in the software. $K_p = 2000$ was found to be sufficient in creating approximately 15% overshoot which is used in order to identify the system which is shown in Figure 2.

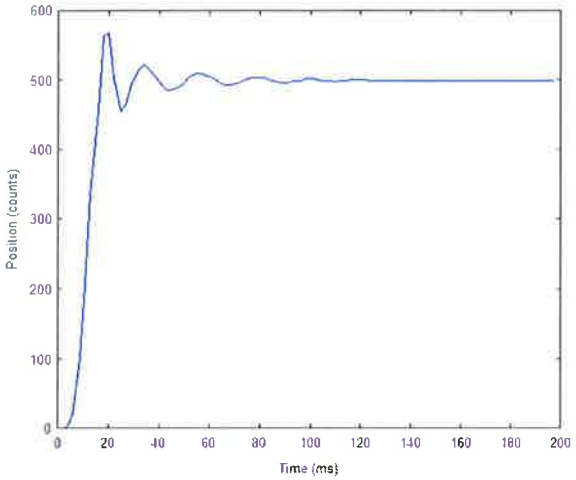

Figure 2 - Step response from SMITuner

From Figure 2 the graph of the step response is jagged due to the low data transfer rate settings of the SMITuner. Thus, a custom script was used to generate a trapezoidal waveform in order to identify the system. Using a least squares approximation, the system's constants were identified, the graphical result of the predicted response is shown in Figure 3.

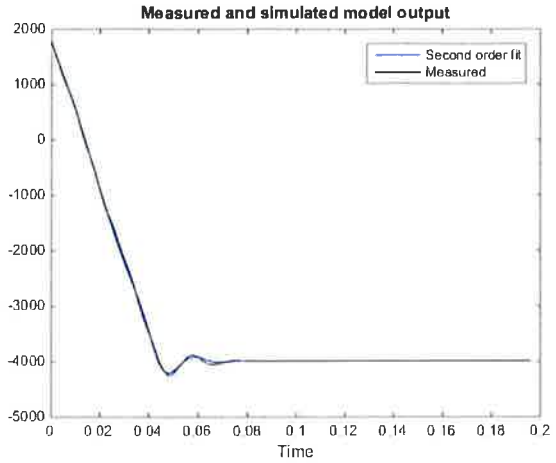

Figure 3 - Second order transfer function fit result

III. Simulation

The model of $P(s)$ was generated in MATLAB in order to use the "pidtool" function. This allowed the specification of bandwidth and phase margin. The key while using this tool was to keep the gain of the system near $K_p = 2000$ to insure the stability of the system. Otherwise, large undamped oscillations might be present. In this case, the phase margin was selected to be 70 degrees, and bandwidth to be 326 rad/s. This is the bandwidth of the system without a spool, which will undoubtedly become much lower as more inertia is added.

At this point, all three values of K_p, K_i, K_d can all be tuned easily using the tuner based on a model of the plant. Only K_a and K_v the acceleration and velocity feed-forward constants must then be specified to complete the controller design.

Fortunately, in the ideal case, selection of $K_a = J_e$ and $K_v = B_e$ is a simple rule that allows excellent system performance if the inertia is constant. Theoretically, this would create a unity gain transfer function, although in practice this is impossible.

As the inertia decreases over time, the performance decays, although not to an unacceptable level. This control scheme is generally known as a 2 DOF controller, note that feeding the velocity and acceleration directly to the control output is only possible because the trajectory generator ensures smoothness of v since acceleration a is specified. If higher performance is necessary, the K_a constant can be modified periodically with the quartic model of inertia to interpolate using radial measurements.

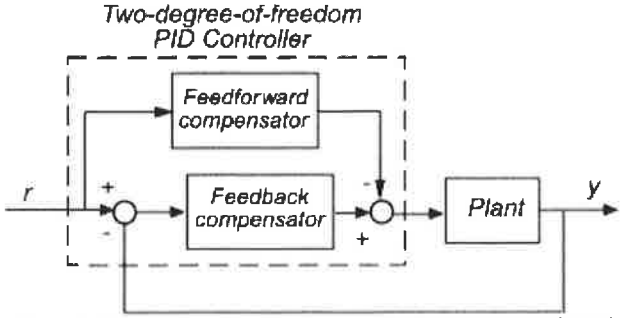

Figure 4 - Schematic of the 2 DOF control scheme from MathWorks

IV. Selection of Trajectory Parameters

The Animatics motor uses a simple trajectory generator that requires the specification of parameters ADT, and VT in order to run in velocity mode. ADT specifies the acceleration and deceleration, while VT sets the cruising velocity. These parameters are easily read off the torque curve of the motor in Figure 5. The red region is where maximum speed operation takes place, notably the reducer was designed to keep the motor operating near the peak power point. This red region has a minimum torque of approximately 0.4Nm at 4000RPM, which means 4Nm at the output of the reducer (which has a predicted 98% of the inertia). Since the velocity is never required to go over 3600RPM, this builds a safety factor into the system in terms of torque and ensures that the velocity cannot go far beyond what is necessary.

$$ADT = \frac{4Nm}{I_{system}}$$
$$\max VT = 4000RPM$$

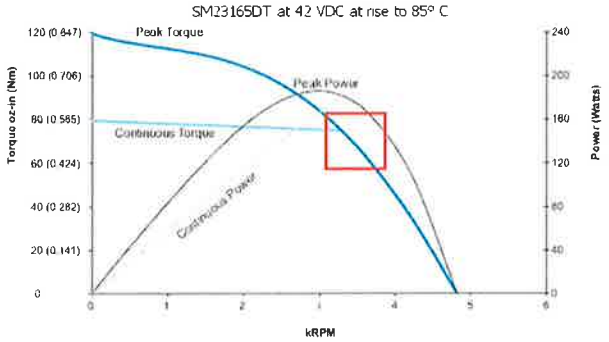

Figure 5 – SM23165DT Torque-speed curve at 42VDC

Preliminary spool motor sizing and high level controller design

Owen Lu
Electroimpact Inc.
owenl@electroimpact.com

***Abstract*—This document details the calculations that were done to estimate the size of motor that can be used to control the dancer system via motors placed on the spool. These calculations take into account the controller response as well as motor specifications. The calculations were then validated by a Bosch IndraDrive system using a pure feedback control scheme to control tow tension.**

I. Introduction

This project has been undertaken in order to remedy tow slack issues in the 777 project. Using servo drives, it is hypothesized that high bandwidth control of the dancer position can be achieved with no tension loss. Subsequently, the tension in the tow can also be controlled to a far greater degree of accuracy, improving consistency and reducing the risk of slack.

II. Kinetmatic derivation

Since the dancer assembly is kinematically similar to a rope pulley system, one can write by inspection that the dancer displacement against the spring is given by Equation (1).

$$x_d = \int \frac{v_o - v_i}{2} dt \tag{1}$$

Where
v_o is the feed velocity
v_i is the tow surface velocity leaving the spool
x_d is the dancer displacement from the initial position

The system can then be written in Laplace domain.

$$x_d(s) = \frac{v_o(s) - v_i(s)}{2s} \tag{2}$$

The intent in this system is to use a pure position feedback to control the dancer position and subsequently tension of the system.

Therefore plant $G(s)$ is defined below in Equation (3) as a pure integrator system.

$$G(s) = \frac{1}{2s} \tag{3}$$

III. Velocity controller design

In general, inertia ratios are used as a rule of thumb to size motors. This is due to the internal drive controller loops being pre-tuned for ease of use such as in the IndraDrive system.
We want to treat a few of these systems in different spool configurations as black boxes and measure the FRF to obtain a quick idea of how far performance can be pushed with minimal dynamics calculations. However, these readings cannot be taken at face value as small signal characteristics do not necessarily translate directly to response of larger signals. Other problems such as saturation and torque limitations will change the response of the system.

Using Bosch Indraworks a FRF can be obtained via the "Frequency Response Analysis" tool. A figure of the output is shown below.

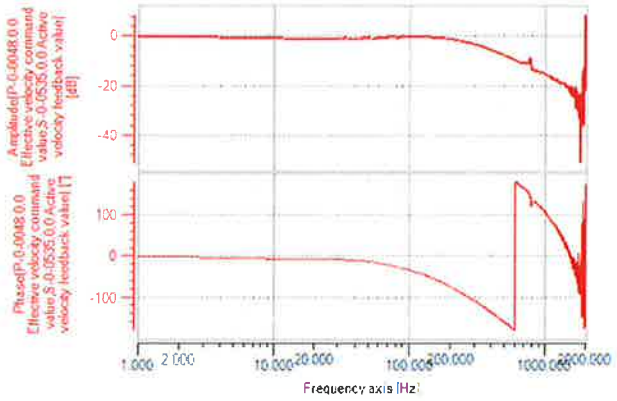

Figure 1 – Bosch Indraworks typical frequency response output

Indraworks software has not unwrapped the angle. The MATLAB unwrap function allows this to be done easily. Figure 2 shows the unwrapped measured response of the velocity loop when the spool and carbon is connected.

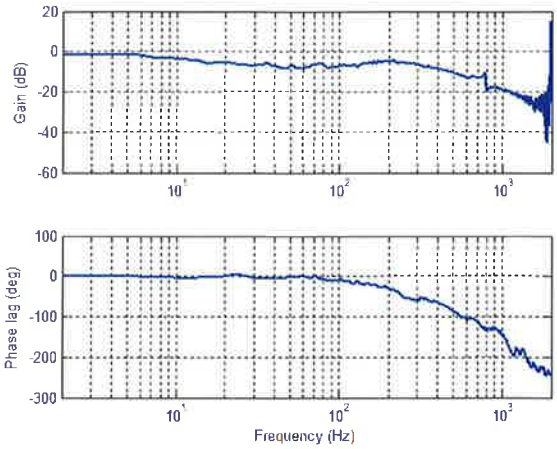

Figure 2 - Unwrapped frequency response

The -3dB bandwidth is near 10Hz using a 4 inch diameter spool of ¼ inch carbon fiber.

The main transfer functions are from the payout surface speed and the displacement dancer reference. Interestingly the payout surface speed is the more important input in terms of dynamic characteristics since x_r is unchanging as a set point (constant tension control). Thus, Equation (4) is of primary interest.

$$\frac{x_d}{v_0} = \frac{s}{2s^2 + K_p r_s s + K_p r_s / T_i} \tag{4}$$

$$\frac{x_d}{x_r} = \frac{K_p r_s s + K_p r_s / T_i}{2s^2 + K_p r_s s + K_p r_s / T_i} \tag{5}$$

Simulation can be done to determine dancer travel based on the momentary ramp input of 0.5G acceleration, and sizing can be conducted.

Since the characteristic equation is second order, it is easy to develop rules of thumb based on measurements r_s to optimize the performance of the system and maintain consistency.

The bandwidth can be calculated below with the simple approximation.

$$\omega_b = \sqrt{\frac{r_s}{2T_i}} \tag{6}$$

Then the damping ratio can also be calculated.

$$\zeta = \sqrt{\frac{r_s K_p T_i}{8}} \tag{7}$$

Therefore specifying ω_b and ζ while simultaneously measuring r_s we can obtain both controller parameters to maintain the same system response in theory. This should be done in context of the system limits, such as drive saturation, and torque limitations which will be discussed in future documents.

IV. Optimal PI controller design

Since packaging is the primary concern in this design, the natural question is what the minimum specification of the motor that can satisfy the design requirements. This is a bit of a simplification, as power density differs from different servo designs, however is sufficient for a first look.

The reason PI controllers are of interest is that they are easy to implement and satisfy the basic requirements of the system. Interestingly, selection of optimal controllers is tied directly to the motor sizing. Thus, the problem can be thought of in two directions.

The problem can be stated below. Given a dancer travel limit l and two cases: step velocity input disturbance at 2000in/s, and 0.5G ramp input disturbance to 4000in/s find the lowest torque requirement. Simulation will be used prove the viability.

Assume that the following process takes place.

1. The system is turned on with some nominal tension in the tow
2. The reference is set and the servo controls the dancer to the reference position via velocity input to the motor
3. After this, one of two scenarios will be realized
    a. Case 1: A step velocity input at the feed is activated at 2000in/min
    b. Case 2: A ramp velocity input at the feed is activated at 0.5G

Although control problems generally wish to shape the response to the reference position to some desired specification, in this application it is far less important than the response to the input disturbance. This is because the process of tensioning before payout can be thought of as initialization since the tension should be constant. However the process of payout causes the dynamic response of x_d which we wish to be constant.

Design of the controller is done for Case 1 which causes the larger disturbance in x_d which is explained later.

Assuming that the tension has reached its initial reference, the payout process begins with a step input of 2000in/min at v_o. The fastest that the surface speed v_i can reach v_o is limited by the maximum torque of the motor T_m.

$$T_m = I_{eq}\alpha_m \tag{8}$$

This means that in the best case, to reach an equilibrium offset, by achieving two equal speeds, the motor is simply turned on, run at maximum torque until no speed difference exists.

The problem can then be reinterpreted, to solve for the controller.

The response of the v_i the tow surface speed can be written as v_o.

$$H(s) = \frac{v_i}{v_o} = \frac{Cr_s}{2s + Cr_s} \tag{9}$$

Using the characteristics of a first order system we can solve for the form of $C(s)$

Let

$$H(s) = \frac{1}{\tau s + 1} \tag{10}$$

Solving for $C(s)$ gives a proportional controller.

$$C(s) = K_p = \frac{2}{\tau r_s} \tag{11}$$

The initial acceleration of v_i is specified by τ since $H(s)$ is first order. Simply setting the acceleration to the acceleration corresponding to maximum torque allows us to limit the dynamic torque on the motor below this value.

$$a_i = \frac{v_i}{\tau} \tag{12}$$

$$r_s \alpha_i = a_i = \frac{v_i}{\tau} \tag{13}$$

$$\alpha_i = \alpha_m = \frac{T_m}{I_{eq}} \tag{14}$$

$$\frac{r_s T_m}{I_{eq}} = \frac{v_i}{\tau} \tag{15}$$

Therefore, proportional gain that maximizes the performance of the dancer response to disturbance input can be written as a function of T_m the maximum torque.

$$K_p = \frac{2T_m}{v_o I_e} \tag{16}$$

Selection of such K_p ensures that torque limits are obeyed. Now the problem becomes the effect of integral action. Recall Equation (7). It is clear that the damping ratio is directly affected by integral time. Written in terms of the integral transition bandwidth ω_I is below.

$$\zeta = \sqrt{\frac{K_p r_s}{8\omega_I}} \tag{17}$$

Therefore, the damping ratio of the response is directly affected by the choice of ω_I, and r_s. The effect of r_s is accounted for later. So the larger ω_I the faster zero error is achieved, however with the more oscillation as a trade off.

Suppose that we set the damping ratio to $\frac{1}{\sqrt{2}}$ which is slightly underdamped.

$$\omega_I = \frac{K_p r_s}{4} \tag{18}$$

At this point all controller parameters are specified by the maximum torque of the motor, the spool radius, and the effective inertia at the spool shaft. Thus, changing the maximum torque, we can see the effect on the performance of the system.

V. Simulation

The simulation was conducted in SciLab an open source software with the following block structure.

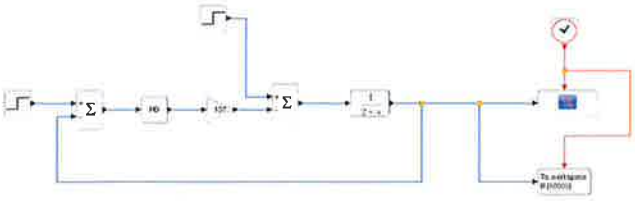

Figure 3 – Initialization and step velocity input simulation

Below is an example simulation comparing the specified PI controller to the optimal bang-bang control to get to cruise velocity as fast as possible.

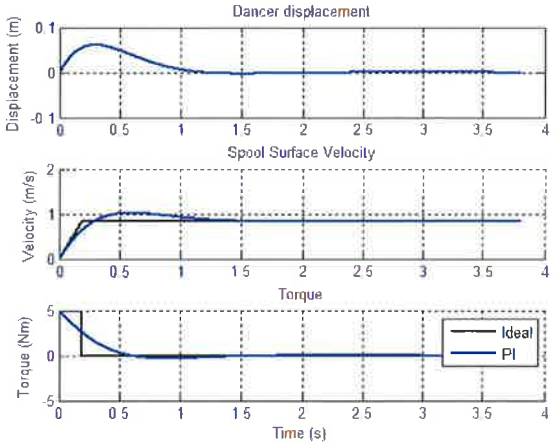

Figure 4 - Optimized PI control vs bang-bang control

Simulation parameters are shown in the Table 1.

Parameter	Magnitude
Maximum torque (Nm)	5
Effective inertia (kgm^2)	0.05
Spool diameter (in)	3.5
Payout velocity (in/min)	2000

Table 1 - Simulation parameters

Below is the simulation of the curve describing trade-off between maximum torque and maximum displacement from equilibrium. In practice, approximately 2in or less is acceptable, for safety we may choose something around 8-12Nm after the reducer to be the output. This number corresponds to the reducer output at peak torque since such a torque is maintained for a very short amount of time.

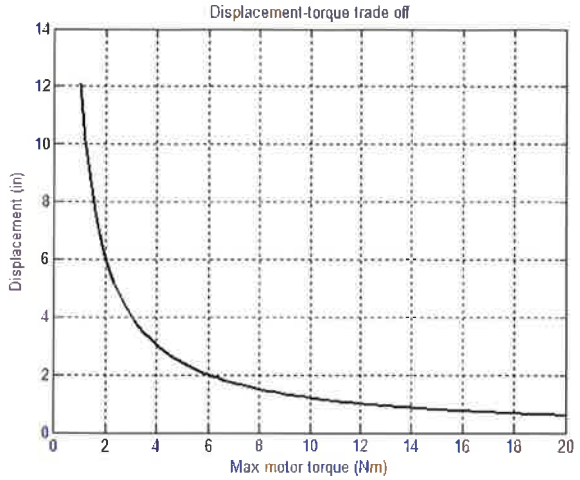

Figure 5 - Displacement amplitude vs. maximum torque

Note that the response of the dancer displacement to the reference displacement is dominated by the same poles as the response to the payout, these do not need to be tuned. However, since a zero exists, we choose a pre-filter to cancel the zero and maintain unity gain.

$$F(s) = \frac{r_s/T_i}{K_p s + r_s/T_i} \tag{19}$$

A sample response choosing 5cm as the reference point is shown below. Notably controller constants are functions of the spool diameter. Thus, performance will vary as time goes on unless the controller parameters are continuously modified with sensor input.

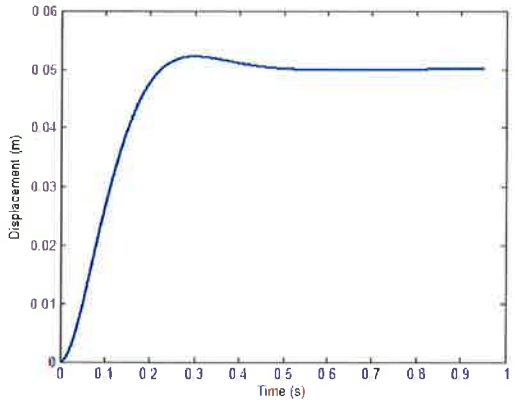

Figure 6 - Step response to dancer displacement input

This analysis concludes that a simple continuous PI controller paired with a properly geared motor can necessarily generate the control signals required to bound dancer displacement and subsequently tension without worry of saturation and exceeding torque limits specified.

VI. Experiment and Theory

A. Step input reference

Notably, the theoretical model which is outline in Figure 3 does not fully describe the process that generates velocity commands. In reality, multiple sub loops exist as well as other trajectory generation related algorithms. Thus, there will be limitations in the model's ability to predict the outcome.

Initially a proportional controller was used by request from upper level management. The dancer position was set at 1in and an approximate step velocity payed out. The graph comparing the theoretical and experimental results is shown in Figure 7.

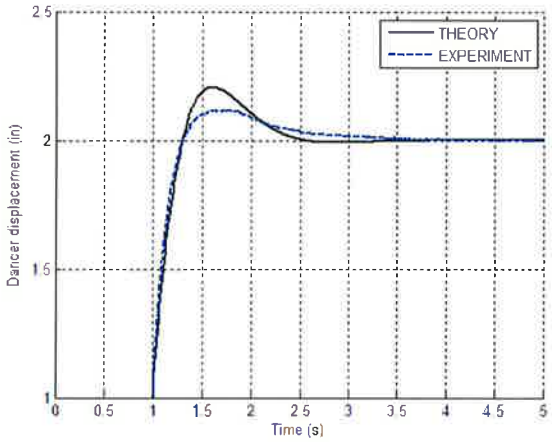

Figure 7 - Step input comparison between model and experiment

The proportional action near the beginning of the step traces the experimental performance almost perfectly, however the integral action is noticeably more damped than expected. This is favorable to the theoretical response, however the reason for this has yet to be identified.

VII. Conclusion

Preliminary testing of the system using Bosch IndraDrive software shows that the motor combined with the tuning method is likely capable of providing sufficient torque for operation. However, with the current internal loop tuning, torque may spike over the rated torque for a small amount of time ~0.1s causing a software fault. More study is necessary to ensure that the software settings are correct and allow safe operation. Possible upgrades to the mechanical system may also be necessary to ensure that the tow is able to payout at proper speeds.